HHS Public Access

Author manuscript

Neurobiol Dis. Author manuscript; available in PMC 2017 July 01.

Published in final edited form as:

Neurobiol Dis. 2016 July ; 91: 209–220. doi:10.1016/j.nbd.2016.03.017.

Role of Histone Acetylation in Long-term Neurobehavioral Effects of Neonatal Exposure to Sevoflurane in Rats

Min Jia[#a], **Wen-Xue Liu**[#a], **Jiao-Jiao Yang**[b], **Ning Xu**[b], **Ze-Min Xie**[b], **Ling-Sha Ju**[a], **Mu-Huo Ji**[a], **Anatoly E. Martynyuk**[c,d], and **Jian-Jun Yang**[a,b]

[a] Department of Anesthesiology, Jinling Hospital, School of Medicine, Nanjing University, Nanjing, China

[b] Jiangsu Province Key Laboratory of Anesthesiology, Xuzhou Medical College, Xuzhou, China

[c] Department of Anesthesiology, University of Florida, Gainesville, Florida, USA

[d] McKnight Brain Institute, University of Florida, Gainesville, Florida, USA

[#] These authors contributed equally to this work.

Abstract

Human studies, and especially laboratory studies, provide evidence that early life exposure to general anesthesia may affect neurocognitive development via largely unknown mechanisms. We explored whether hippocampal histone acetylation had a role in neurodevelopmental effects of sevoflurane administered to neonatal rats. Male Sprague-Dawley rats were exposed to 3% sevoflurane or were subjected to maternal separation only for 2 h daily at postnatal days 6, 7, and 8. The histone deacetylase inhibitor, sodium butyrate (250 mg/kg, intraperitoneally), or saline was administered starting 2 h prior to anesthesia or maternal separation and continued daily until the end of behavioral tests, which were performed between postnatal days 33 and 50. Upon completion of the behavioral tests, the brain tissues were harvested for further analysis. Rats neonatally exposed to sevoflurane exhibited decreased freezing time in the fear conditioning contextual test and increased escape latency, decreased time in target quadrant, and number of platform crossings in the Morris water maze test. The sevoflurane-exposed rats had lower hippocampal density of dendritic spines, reduced levels of the brain-derived neurotrophic factor, c-fos protein, microtubule-associated protein 2, synapsin1, postsynaptic density protein 95, pCREB/CREB, CREB binding protein, and acetylated histones H3 and H4, and increased levels of histone deacetylases 3 and 8. These neurobehavioral abnormalities were normalized in the sevoflurane-

Address correspondence to Dr. Yang, Department of Anesthesiology, Jinling Hospital, 305 East Zhongshan Road, Nanjing 210002, China. yjyangjj@126.com and Prof Martynyuk, Department of Anesthesiology, University of Florida, 1600 SW Archer Road, PO Box 100254, Gainesville, FL 32610, USA. amartynyuk@anest.ufl.edu.

Department/institution to which the work is attributed: Department of Anesthesiology, Jinling Hospital, School of Medicine, Nanjing University

There are no conflicts of interest.

Meetings at which the work has been presented: None

exposed rats treated with sodium butyrate. Our findings provide evidence that neonatal exposure to sevoflurane induces neurobehavioral abnormalities and long-lasting alterations in histone acetylation; normalization of histone acetylation may alleviate the neurodevelopmental side effects of the anesthetic.

Keywords

Neonatal rats; Sevoflurane; Maternal separation; Hippocampus; Histone acetylation; Synaptic plasticity

Introduction

Most of human retrospective epidemiological analyses and a rapidly increasing number of specifically designed laboratory studies provide evidence that general anesthesia, administered during the early period after birth, may induce developmental neurocognitive abnormalities that can be detected long after the anesthesia exposure (Wilder et al., 2009; Edwards et al., 2010; Sun, 2010; Seubert et al., 2013; Shen et al., 2013; Rappaport et al., 2015; Xu et al., 2015). Given that millions of newborns and young children are exposed to general anesthesia every year, the possibility that a clinical procedure may have long-lasting deleterious effects on brain development in our youngest patients is an issue of important health concern (Servick K., 2014; Rappaport et al., 2015). The only way to address this is to develop safer anesthesia because treatment of many life-threatening conditions requires general anesthesia. Poor understanding of the mechanisms mediating adverse developmental effects of general anesthetics is an important barrier on the way to developing safer anesthesia.

A rapidly raising number of studies demonstrate that epigenetic mechanisms, such as DNA methylation and histone acetylation, are involved in the mediation of environmental factor-induced shaping of the developing brain during its critical period of maturation by reprogramming diversified gene expression, some of which can also be seen as differential in early brain development (Fischer et al., 2007; McClelland et al., 2011; Powell and LaSalle, 2015; Roth and Sweatt, 2011; Johnson et al., 2009). These mechanisms are critical mediators whereby early life environmental factors affect long-term learning and memory, resulting in improvement of mental function or neuropsychiatric disorders. During general anesthesia, anesthetic agents such as sevoflurane force transition of the brain into a coma state that is characterized by profound alteration of most aspects of brain functioning (Baker et al., 2014; Franks and Zecharia, 2011), placing general anesthetic agents among highly reactive environmental factors. The importance of environmental factors in the developmental outcome of neonatal anesthesia in rodents is evident from the opposite effects of postanesthesia enriched and deprived housing conditions (Brenes et al., 2015; Shih et al., 2012; Zhang et al., 2015). Therefore, it is plausible that general anesthetics may initiate developmental abnormalities in the brain, at least in part, through modulation of epigenetic mechanisms. This possibility is further supported by the fact that neurotrophins such as brain-derived neurotrophic factor (BDNF), which plays an important role in brain development and function, and which is shown to be involved in the neurodevelopmental

effects of neonatal anesthesia (Head et al., 2009), are downward targets for regulation by histone acetylation (Barichello et al., 2015; Khan and Jena, 2014; Sharma, 2010). Histone acetyltransferases and histone deacetylases (HDAC) modulate histone interaction with DNA by adding and removing acetyl groups to N-terminal of histone tails, respectively. Histone acetyltransferases can enable chromatin relaxation and facilitate transcription, whereas HDAC enable chromatin compaction and repress transcription (Bannister and Kouzarides, 2011; Fischer et al., 2010; Guan et al., 2009; Jia et al., 2015; McQuown et al., 2011). In the present study, we investigated whether early life exposure to sevoflurane anesthesia-induced neurobehavioral abnormalities in rodents are associated with alterations in hippocampal histone acetylation and whether such neurobehavioral abnormalities can be ameliorated by treatments with the HDAC inhibitor, sodium butyrate (NaB) (Intlekofer et al., 2013; Febo et al., 2009; Fontan-Lozano et al., 2008; Khan and Jena, 2014; Rane et al., 2012).

Materials and Methods

Animals

The present study was approved by the Ethics Committee of Jinling Hospital, Nanjing University, China, and was performed in accordance with the Guide for the Care and Use of Laboratory Animals from the National Institutes of Health (Bethesda, Maryland). Sprague-Dawley rats (dams with pups) were purchased from the Animal Center of Jinling Hospital, Nanjing, China, and were housed individually in standard conditions with a 12-h light/dark cycle (light from 07:00–19:00) at 23 ± 1°C and *ad libitum* access to food and water. At the age of 21 days, pups were weaned and housed in sex-matched groups of three to four for the rest of the study. To control for litter variability, several pups from different litters were used for each treatment condition. The data reported in this study was collected from 60 male rats.

Sevoflurane Exposure

The P6 male rat pups were randomly assigned to be exposed to sevoflurane or not exposed to sevoflurane. Rats received 3% sevoflurane in O_2 for 2 h daily for three consecutive days in a thermostat chamber set to 37 ± 1ºC (Shen et al., 2013). The total gas flow was 1.5 L/min. The rats breathed spontaneously, and concentrations of anesthetic and oxygen were measured continuously using a calibrated Datex side stream analyzer (Vamos, Drägerwerk AG & Co., Shanghai, China) that sampled from the interior of the animal chamber. After termination of anesthesia, the rat pups recovered with the thermostat set at 37 ± 1°C. Upon gaining the righting reflex, the pups were returned to the mothers. The animals not exposed to sevoflurane were separated from the dams for the same duration of time in a temperature-controlled chamber with a continuous supply of oxygen. In line with previous studies (Lu et al., 2010; Shen et al., 2013), we found that anesthesia with 3% sevoflurane for 2 h did not significantly change the values of pH, partial pressure of oxygen, and/or carbon dioxide compared to the control group.

Drug Treatment

To study the role of histone acetylation in the developmental effects of sevoflurane, the inhibitor of HDAC, NaB (250 mg/kg, intraperitoneally, i.p.), was administered to

sevoflurane (Sev)-exposed (the Sev + NaB group) and sev-non-exposed, that is, the maternal separation (MS) + NaB group rats. To control for the injections, an equal volume of i.p. saline, the vehicle for NaB, was administered to another half of sevoflurane-exposed (the Sev group) and sevoflurane-non-exposed (the MS group) rats. The injections were done 2 h prior to anesthesia with sevoflurane or MS and then daily until the end of behavioral tests at P50 (Fig. 1). The i.p. injections were alternated daily between the right and left sides of the abdomen. The volume of injection was 10 ml/kg. All rats were sequentially evaluated in open field (OF) tests starting at P33, Morris water maze (MWM) tests starting at P36, and fear conditioning (FC) tests starting at P48 (Fig. 1).

Behavioral Tests

All apparatus used to conduct the behavioral tests were purchased from Shanghai Softmaze Information Technology Co. Ltd, Shanghai, China. All behavioral tests were performed during the light phase of a 12-h light/dark cycle between 9:00 A.M. and 4:00 P.M.

OF Test—Explorative activities and anxiety-like behaviors were studied by using the OF apparatus (XR-XZ301). The rat was placed in a gray plastic chamber (100 cm × 100 cm × 40 cm) and was allowed to explore the apparatus for 10 min; this autonomous exploration was automatically recorded by a video tracking system. After each test, the surface of the apparatus was thoroughly cleaned with 75% alcohol to avoid the presence of olfactory cues from the previous rat.

MWM Test—Spatial learning and memory of the rats were tested by using the MWM apparatus (XR-XM101). The apparatus was consisted of a circular tank (150-cm diameter, 55-cm height) filled with water (35 cm, approximately 23 ± 1°C. The pool was surrounded with an opaque curtain and was placed in an isolated room with four visual cues on the wall of the tank. A nontoxic paint was used to render the water opaque. The tank was divided into four equal quadrants, labeled left-top, left-bottom, right-top, and right-bottom. A 10-cm diameter platform (as the escape platform) was submerged 1.5 cm below the surface of the water at a constant location in one of the quadrants, *i.e.*, the left-top quadrant in this study. The rats were tested in the MWM four times per day for six consecutive days from P36 to P41 to search for the escape platform (Fig. 1). The starting points for each rat were randomly chosen in one of the four quadrants, and the each trial had a ceiling time of 60 s or a stopping time of when the escape platform was found. Between the trials, the rat was allowed to stay on the platform for additional 15 s to rest. If the rat failed to find the platform within 60 s, it was gently guided to the platform and allowed to rest on the platform for additional 15 s prior to the next trial. A video tracking system recorded the swimming tracks of the rats. Twenty-four hours later, on P42, the spatial memory test was performed. The test lasted 60 s, during which the escape platform was removed. The rat was placed in the tank in the contralateral quadrant relative to the original location of the escape platform (the target quadrant). The time spent in the target quadrant and the number of times the rat crossed the previous location of the escape platform were recorded.

FC Test—The rats were put in the training chamber (32 cm × 32 cm × 45 cm) with 21 stainless steel rods evenly distributed at the bottom of chamber. The chamber was placed in

a soundproof box (52 cm × 45 cm × 75 cm) with a camera fixed on the top. The rats were habituated to the chamber for 180 s, after which they received a tone stimulus (30 s, 70 dB, 3000 Hz) followed by an electric foot-shock (2 s, 0.7 mA) delivered during the last 2 s of the tone stimulus. After the foot-shock, the rats remained in the chamber for an additional 30 s before being returned to their home cages. Twenty-four hours later, a contextual FC test was performed. The rats were returned to the original training chamber and allowed to explore the context for 300 s without any stimulation. Forty-eight hours after the FC training, a cued FC test was performed. The rat was placed into a novel chamber (with a smooth flat rather than a grid floor, and altered color, shape, materials, and smell) for 180 s for habitation followed by the 180 s of the training tone (70 dB, 3000 Hz). Activities were tracked using a video tracking system. The percentage of time spent freezing was used to measure the fear memory formation after training. Freezing was defined as no movement with the exception of respiration for at least 1 s. The chamber was thoroughly cleaned with 75 % alcohol at the end of each training and testing.

Isolation of the Hippocampus

One hour after a cued FC test, five rats from each experimental group were sacrificed by administering sodium pentobarbital (60 mg/kg, i.p.) followed by decapitation. The hippocampus was dissected as described elsewhere (Kilgore et al., 2010), placed in liquid nitrogen, and stored at −80 °C.

Preparation for Hippocampal Protein Extractions

For histone extraction, the tissue samples were homogenized in ice-cold solution containing (in millimoles): 50 Tris-HCl, 25 KCl, 250 sucrose, 2 NaB, 1 sodium orthovanadate, 0.5 phenylmethylsulfonyl fluoride, and 1× protease inhibitor cocktail, pH 7.5. The tissue homogenates were centrifuged at 7700 *g* for 60 s at 4 °C. The supernatant was aspirated and the pellet was resuspended in 1 ml 0.4 N H_2SO_4. Trichloroacetic acid with 10 mM sodium deoxycholate was added to the supernatant for 30 min at 4°C to extract histones, followed by centrifugation at 14000 *g* for 30 min. The protein pellet was washed once by acidified acetone (0.1% HCl) for 5 min. Protein pellets were collected between washes by centrifugation at 14000 *g* for 5 min and were then resuspended in 50 mM Tris-HCl (pH 8.0) and stored at −80 °C.

For measuring the proteins of HDAC1, HDAC2, HDAC3, HDAC8, BDNF, c-fos, microtubule-associated protein 2 (MAP2), synapsin1, PSD95, cyclic-AMP response element binding protein (CREB), phosphrated-CREB (pCREB), and CREB binding protein (CBP) in the hippocampus, radioimmunoprecipitation assay buffer containing 1× protease inhibitor cocktail was used. Homogenates were centrifuged at 13000*g* at 4°C for 10 min and the supernatants were transferred to a fresh tube for western blotting.

Western Blot

Five rats in each group were used for western blot. Levels of hippocampal HDAC1, HDAC2, HDAC3, HDAC8, total-H3, acetyl-H3K9, acetyl-H3K14, total-H4, acetyl-H4, acety-H4K5, acetyl-H4K12, BDNF, c-fos, MAP2, synapsin1, PSD95, pCREB/CREB, and CBP were assayed by the western blot. The hippocampus was homogenated in

radioimmunoprecipitation assay buffer plus protease inhibitors (Sigma, St. Louis, Missouri), and centrifuged at 4°C for 15 min at 12000 rpm; the supernatant was then collected. The protein concentrations were measured according to the method of Bradford using bovine serum albumin as a standard (BioRad, Hercules, California). Protein extracts (20 μg/well) were separated by sodium dodecyl sulfate polyacrylamide gel electrophoresis (SDS-PAGE) on 8% to −12% resolving gels and were then transferred to polyvinylidene difluoride membranes. After that, the membranes were incubated in primary antibody containing Tris-buffered saline and Tween 20 (TBST) and 5% nonfat dry milk for 60 min at room temperature. The following anti-rabbit, anti-rat, or anti-mouse primary antibodies were used as follows overnight at 4°C.: anti-HDAC1 (1:1000; Abcam, Cambridge, UK), anti-HDAC2 (1:1000; Abcam), anti-HDAC3 (1:1000; Abcam), anti-HDAC8 (1:1000; Abcam), anti-histone H3 (1:500; Cell Signaling, MA, USA), anti-histone H3 (acetyl K9) (1:500; Abcam), anti-histone H3(acetyl K14) (1:500; Abcam), anti-histone H4 (1:500; Cell Signal Technology, Danvers, Massachusetts), anti-acetyl histone H4 (Lys5/8/12/16) (1:500; Abcam), anti-histone H4 (acetyl K5) (1:500; Abcam), anti-histone H4 (acetyl K12) (1:500; Abcam), anti-BDNF (1:1000; Santa Cruz Technologies, Santa Cruz, California), anti-c-fos (1:500; Santa Cruz Technologies), anti-MAP2 (1:1000; Abcam), anti-Synapsin1 (1:1000; Merck Millipore, Darmstadt, Germany), anti-PSD95 (1:1000; Abcam), anti-CREB (phospho S133) (1:500; Abcom), anti-CREB (1:500; Abcom), and anti-CBP (1:500; Cell Signaling). After three washings with TBST for 5 min, membranes were incubated in 5% nonfat dry milk in TBST and incubated in the secondary antibodies (1:10,000; goat anti-rabbit or goat anti-mouse; 1:5000, goat anti-rat; Bioworld Technology, Nanjing, Jiangsu, China) for 60 min at room temperature. The membranes were rinsed again in TBST three times for 5 min. Enhanced chemiluminescent and Image J software (Version 1.49v, NIH, Bethesda, Maryland) were used to visualize and quantitate the bands, respectively.

Immunofluorescence

Six rats in each group were used for the immunofluorescence analysis. One hour after completion of the cued FC test, rats were anesthetized with sodium pentobarbital (60 mg/kg, i.p.). The anesthetized rats were perfused transcardially via the left ventricle with 200 ml of phosphate-buffered saline (PBS; pH 7.4), followed by 300 ml of 4% paraformaldehyde in PBS (pH 7.4). The brains were harvested and dipped in 4% paraformaldehyde at 4°C for 2 h, dehydrated in 30% sucrose for 24 h, embedded with OCT (Leica, Jung, Germany), and stored at −80°C. Coronal sections (10 μm thick) were cut from −2.12 to −4.80 mm of the bregma using the frozen section machine (Leica CM 1950). The sections were rinsed with PBS three times for 5 min to wash off the OCT, mounted with 10% normal goat serum for 1 h at room temperature, and then incubated with anti-histone H3 (acetyl K9; 1:500; Abcam), anti-histone H3 (acetyl K14; 1:500; Abcam), anti-histone H4 (acetyl K5; 1:500; Abcam), or anti-histone H4 (acetyl K12; 1:500; Abcam) overnight at 4 °C. The sections were washed with PBS three times for 5 min and incubated at room temperature for 1 h with the second antibody (goat anti-rabbit; 1:300; Bioworld Technology, Nanjing, Jiangsu, China) and 4',6-diamidino-2-phenylindole (1:1000; Sigma). After repeated washing with PBS, the sections were mounted with 50% glycerine. Fluorescence FV-1000 confocal microscope (Olympus, Japan) was used under 200× magnification to acquire images of the hippocampus.

Golgi Staining

Four rats in each group were used for Golgi staining analysis. Golgi staining was performed using an FD Rapid GolgiStain™ Kit (FD Neurotechnologies, Inc., Columbia, Maryland). The rats were sacrificed with an overdose of sodium pentobarbital (60 mg/kg, i.p.). The brains were harvested and the hippocampus was immediately dissected, rinsed in Milli-Q water to wash blood from the surface, and then immersed in FD Rapid Golgi staining impregnation solution, including solution A and solution B (volume 1:1) for 21 d. The impregnation solution was replaced after 24 h. Later, the tissue was transferred into solution C, which was replaced after 24 h, and stored at 4ºC in the dark for 7 d. The 120-μm-thick tissue slices were cut using a vibratome. The tissue slices were transferred on gelatin-coated microscope slides with solution C. The sections were allowed to dry naturally and stored in a slide box at room temperature in the dark for 3 d. After that, the sections were washed with Milli-Q water two times for 2 min. The sections were then placed in a mixture containing 1 part solution D, 1 part solution E, and 2 parts Milli-Q water. Ten minutes later, the sections were washed with Milli-Q water again two times for 4 min and dehydrated using graded ethanol (50%, 75%, and 95%, respectively), each time for 4 min. The tissue sections were dehydrated again using absolute ethanol four times for 4 min prior to permeabilization with xylene three times for 4 min. Finally, the sections were covered by cover slides with permount TM mounting medium. The pictures of pyramidal neurons in the hippocampal CA1 subfield were taken using an Olympus FV1000 confocal microscope (Olympus, Japan) at 400× magnification. The pictures of dendritic spines were visualized using a BM53F microscope (Olympus) under oil immersion at a 1000× magnification. The quantification of dendritic branching points and intersections was performed using Sholl analysis (version v3.4.4, NIH, Bethesda, MD). Dendritic branching and intersections were observed up to the length of a 250 μm distance from the soma center, confirming that apical dendrites can receive major afferent input. In Sholl analysis, concentric circles of 50 μm distances apart were drawn using a stage micrometer scale on the tracks, keeping the center of the soma as the center of concentric circles (Bindu et al., 2007 and Wang et al., 2013a). The number of branching points and intersections was calculated in each successive concentric segment. The length of the apical dendrite was measured using image analysis software NIH Image J ver.1.42 (NIH, Bethesda, MD). The number of dendritic spins was counted using Image J software (version 1.49v).

Statistical Analysis

Data are presented as the mean ± SEM. Statistical analyses were carried out using SPSS software (version 17.0, SPSS Inc., Chicago, IL). Normal distribution of data was analyzed using the Kolmogorov-Smirnov test. Multiple comparisons among groups were analyzed using analysis of variance (ANOVA) followed by the *post hoc* Tukey's test. Two-way RM ANOVA was used to analyze the MWM escape latency data, with the time and treatment as interaction factors (Vorhees and Williams, 2006). The Bonferroni test was used to analyze the difference among experimental groups in escape latency during the MWM training. The dendritic branching points and intersections were also analyzed using two-way RM ANOVA followed by the *post hoc* Tukey's test. A P value less than 0.05 was considered statistically significant.

Results

Rats Exposed to Sevoflurane Neonatally Exhibited Abnormal behavior; Ameliorating Effect of NaB

One-way ANOVA revealed no differences among the four experimental groups during the OF test in the distance traveled ($F_{(3,56)} = 0.183$, $P = 0.908$; Fig. 2A), speed ($F_{(3,56)} = 0.239$, $P = 0.869$; Fig. 2B), and time spent in the center ($F_{(3,56)} = 0.209$, $P = 0.889$; Fig. 2C).

In the MWM test, the rats in the Sev group exhibited longer escape latency on P38 ($F_{(3,56)} = 11.305$, $P < 0.001$; Fig. 2D) and P39 ($F_{(3,56)} = 7.242$, $P < 0.001$; Fig. 2D), spent less time in the target quadrant ($F_{(3,56)} = 9.066$, $P < 0.001$; Fig. 2E), and made fewer platform crossings ($F_{(3,56)} = 6.607$, $P = 0.001$; Fig. 2F). The MWM behavior of the rats from the Sev + NaB group and of the rats not exposed to sevoflurane neonatally was not different (Fig. 2, D-F, $P > 0.05$).

In the FC test, no significant difference was observed during the FC training among the four experimental groups ($F_{(3,56)} = 0.623$, $P = 0.603$; $F_{(3,56)} = 0.463$, $P = 0.709$; Fig. 2G). However, the rats in the Sev group exhibited shorter freezing times in the FC contextual test ($F_{(3,56)} = 12.360$, $P < 0.001$, Fig. 2H), but not in the FC cued test ($F_{(3.56)} = 0.341$, $P = 0.795$, Fig. 2I). Treatments with NaB reversed the effects of sevoflurane on the rat's behavior in the FC contextual test (Fig. 2H).

Hippocampal Levels of HDAC3 and HDAC8 Were Elevated in the Sev Group, But Not in the Sev + NaB Group

No significant difference was found in the levels of hippocampal HDAC1 and HDAC2 among the four experimental groups ($F_{(3,16)} = 0.242$, $P = 0.866$; $F_{(3,16)} = 0.266$, $P = 0.849$; Fig.3A). However, the levels of hippocampal HDAC3 ($F_{(3,16)} = 5.226$, $P = 0.010$; Fig. 3B) and HDAC8 ($F_{(3,16)} = 6.530$, $P = 0.004$; Fig. 3C) in the Sev group were significantly increased. The sevoflurane-exposed rats that were treated with NaB had levels of hippocampal HDAC3 and HDAC8 not different from those in rats that were not exposed to sevoflurane neonatally.

Hippocampal Levels of Histone Acetylation Were Lower in the Sev Group, But Not in the Sev + NaB Group

Assessment of acetylated hippocampal histones in the four treatment groups using western blot found decreased levels of acetyl-H3K9 ($F_{(3,16)} = 4.899$, $P = 0.013$; Fig. 4A), acetyl-H3K14 ($F_{(3,16)} = 7.372$, $P = 0.003$; Fig. 4A), acetyl-H4 ($F_{(3,16)} = 10.237$, $P = 0.001$; Fig. 4B), acetyl-H4K5 ($F_{(3,16)} = 15.154$, $P < 0.001$; Fig. 4B), and acetyl-H4K12 ($F_{(3,16)} = 11.982$, $P < 0.001$; Fig. 4B) in the Sev group. In contrast, these parameters in the sevoflurane-exposed rats treated with NaB were not different from those in rats that were not exposed to sevoflurane (Fig. 4).

Decrease in Hippocampal Levels of Histone Acetylation in Rats Neonatally Exposed to Sevoflurane Was Most Prominent in the CA1 Region

Immunofluorescent staining revealed that the Sev group had lower intensities associated with acetyl-H3K9 ($F_{(3,20)} = 23.103$, $P < 0.001$; Fig. 5), acetyl-H3K14 ($F_{(3,20)} = 21.182$, $P < 0.001$; Fig. 6), acetyl-H4K5 ($F_{(3,20)} = 5.281$, $P = 0.008$; Fig. 7), and acetyl-H4K12 ($F_{(3,20)} = 23.431$, $P < 0.001$; Fig. 8) in the hippocampal CA1 region. There were no significant differences between intensities associated with acetyl-H3K9 ($F_{(3,20)} = 0.387$, $P = 0.763$, Fig. 5), acetyl-H3K14 ($F_{(3,20)} = 0.203$, $P = 0.893$, Fig. 6), acetyl-H4K5 ($F_{(3,20)} = 0.283$, $P = 0.837$, Fig. 7), and acetyl-H4K12 ($F_{(3,20)} = 0.288$, $P = 0.834$, Fig. 8) in the CA3 hippocampal region among the four experimental groups. Similar to the CA3 region, there was no significant difference between intensities of acetyl-H3K9 ($F_{(3,20)} = 0.216$, $P = 0.884$, Fig. 5), acetyl-H4K5 ($F_{(3,20)} = 0.190$, $P = 0.902$, Fig. 7), and acetyl-H4K12 ($F_{(3,20)} = 0.219$, $P = 0.882$, Fig. 8) in the hippocampal dentate gyrus (DG) regions of the four experimental groups. However, the acetyl-H3K14 intensity was decreased in the DG region in the Sev group ($F_{(3,20)} = 41.249$, $P < 0.001$; Fig. 6). The acetyl-H3K9, acetyl-H3K14, acetyl-H4K5, and acetyl-H4K12 intensities had no significant difference in all three hippocampal regions in the Sev + NaB group compared with the non-exposed sevoflurane groups (Figs. 5-8).

Treatment with NaB Normalized Hippocampal Levels of BDNF, c-fos, MAP2, synapsin1, PSD95, pCREB/CREB, CBP, and Density of Dendritic Spines, Reduced by Neonatal Exposure to Sevoflurane

The hippocampal levels of BDNF ($F_{(3,16)} = 22.715$, $P < 0.001$; Fig. 9A), c-fos ($F_{(3,16)} = 8.313$, $P = 0.001$; Fig. 9B), MAP2 ($F_{(3,16)} = 10.297$, $P = 0.001$; Fig. 9C), synapsin1 ($F(3,16) = 6.975$, $P = 0.003$; Fig. 9C), PSD95 ($F_{(3,16)} = 5.017$, $P = 0.012$; Fig. 9C), pCREB/CREB ($F(3,16) = 7.787$, $P = 0.002$; Fig. 9D), and CBP ($F(3,16) = 21.241$, $P < 0.001$; Fig. 9E), were decreased in the Sev group. The levels of these proteins in rats exposed to sevoflurane and treated with NaB were not different from those in rats not exposed to sevoflurane neonatally (Fig. 9).

The Golgi staining technique was used to study the effects of neonatal sevoflurane and treatment with NaB on neuronal dendritic branching points, intersections, length of apical dendrites, and spine density in the hippocampal CA1 region. No significant differences were found in the dendritic branching points ($F_{(3,12)} = 1.20$, $P = 0.352$; $F_{(3,12)} = 0.613$, $P = 0.620$; $F_{(3,12)} = 0.588$, $P = 0.634$; $F_{(3,12)} = 0.769$, $P = 0.533$; $F_{(3,12)} = 0.478$, $P = 0.703$; Fig. 10, A and B), intersections ($F_{(3,12)} = 3.305$, $P = 0.057$; $F_{(3,12)} = 2.452$, $P = 0.114$; $F_{(3,12)} = 0.535$, $P = 0.667$; $F_{(3,12)} = 0.355$, $P = 0.787$; $F_{(3,12)} = 0.606$, $P = 0.624$; Fig. 10, A and C), and length of apical dendrites ($F_{(3,12)} = 0.455$, $P = 0.719$; Fig. 10, A and D) among the four experimental groups. However, dendritic spine density was significantly reduced in the Sev group ($F_{(3,12)} = 7.117$, $P = 0.005$; Fig. 10E). Dendritic spine density in the Sev + NaB group was not different from the same parameters in rats that were not exposed to sevoflurane.

Discussion

The results of this study demonstrate that juvenile male rats exposed neonatally to sevoflurane, one of most frequently used general anesthetics in pediatric anesthesia,

exhibited impaired hippocampus-dependent spatial and associative memory. These behavioral abnormalities were accompanied by reduced spine density and acetylated histones H3 and H4 in the hippocampal CA1 region, as well as decreased levels of hippocampal BDNF, c-fos, MAP2, synapsin1, PSD95, PCREB/CREB, and CBP, and increased levels of HDAC 3 and 8. The levels of acetylated histones, BDNF, MAP2, c-fos, pCREB/CREB, CBP, synaptic proteins, and dendritic spine density, and behavioral characteristics found in sevoflurane-exposed rats treated with the HDAC inhibitor, NaB, were not different from those in sevoflurane-non-exposed rats. These findings suggest that neonatal sevoflurane-induced alterations in epigenetic mechanisms, specifically, an increase in histone deacetylation, are involved in mediation of the developmental neurocognitive effects of the anesthetic. This is in line with a notion that epigenetic mechanisms, histone acetylation in particular, regulate diverse aspects of nervous system development and function, such as dendritic development, synapse maturation, synaptic plasticity, learning, and memory (Fontan-Lozano et al., 2008; Gräff and Tsai, 2013; Graff and Mansuy, 2008; Jarome and Lubin, 2014; Jia et al., 2015; Pirooznia and Elefant, 2013).

Our current findings of neonatal sevoflurane-induced neurodevelopmental abnormalities in rodents are in agreement with the reports from different laboratories (Chung et al., 2015; Wang et al., 2013b; Tan et al., 2014; Xu et al., 2015). The new aspect of these findings is a demonstration that repeated exposures to sevoflurane during the early postnatal period initiate changes in histone acetylation in specific regions of the brain, such as the hippocampal CA1 area, affecting some aspects of rat brain maturation and behaviors, but not others. Thus, sevoflurane-exposed rats exhibited impaired hippocampus-dependent spatial and associative memory. On the other hand, explorative behaviors in the OF test and freezing time in the cued FC test were not different from the MS groups. Treatment with NaB normalized the sevoflurane-induced alterations in hippocampal synaptic morphology as well as the rat's behavior, further implying that histone deacetylation may play a mechanistic role in the observed abnormalities.

We found that NaB, administered to sevoflurane-exposed rats, preserved not only hippocampal synaptic morphology and higher brain activities, *e.g.*, learning and memory, but also reestablished the expression of a number of important brain proteins, including CBP, pCREB/CREB, synaptic protein PSD95 and BDNF, which enhances synaptic plasticity by triggering functional and structural changes in neurons and synapses essential for learning and memory processes (Kellner et al., 2014; Sakata et al., 2013). It was previously reported that exposure of neonatal mice to isoflurane for 4 h resulted in the loss of hippocampal dendritic spines and synapses presumably due to the increase in the pro-BDNF/BDNF ratio (Head et al., 2009), although other investigators did not detect changes in hippocampal BDNF expression after a single exposure of P7 mice to sevoflurane for 2 h (Han et al., 2015). Our findings that treatment with NaB prevented a sevoflurane-induced decrease in hippocampal BDNF expression are in agreement with emerging evidence indicating that histone acetylation/deacetylation modulates BDNF and its role in neurocognitive mechanisms. For example, NaB or voluntary exercise improved performance in the spatial memory task of sedentary mice by upregulating hippocampal BDNF expression (Intlekofer et al., 2013). It is of relevance that recent studies report that neurocognitive developmental abnormalities in neonatal anesthesia exposed-rodents housed

in an enriched environment that included voluntary exercise were largely ameliorated (Brenes et al., 2015; Shih et al., 2012). On the other hand, rats housed in enrichment-deprived conditions exhibited exacerbated neurobehavioral deficiencies (Zhang et al., 2015). Our findings, in combination with data in the literature, support the notion that a chain of events consisting of sevoflurane-induced histone deacetylation, a decrease in hippocampal levels of CBP, pCREB/CREB, and BDNF, and impairment in synaptic integrity could contribute to the observed long-term neurobehavioral effects of the anesthetic in rodents.

The absence of the effects of NaB on behavioral parameters not affected by sevoflurane and the absence of the effects of NaB on sevoflurane-sensitive parameters in rats that were not exposed to sevoflurane, e.g., spatial learning and memory and associative memory, may suggest that a limited number of injections of NaB at the time of exposure to sevoflurane may be as effective as daily injections of the drug during the entire duration of the experiment used in this study. The daily schedule of treatment with NaB in this study was chosen to test in principle whether histone acetylation/deacetylation is involved in developmental neurocognitive effects of neonatal exposure to sevoflurane. It will be important to repeat these experiments in the future using a shorter period of NaB administration after termination of exposure to the anesthetic, as well as lower doses of NaB and other HDAC inhibitors, although chronic NaB treatment was commonly used in the studies of neurodegenerative disease, like Alzheimer's disease (Cuadrado-Tejedor et al., 2013; Dash et al., 2009; Kilgore et al., 2010; Ricobaraza et al., 2012). As far as later is concerned, NaB at the dose that was investigated in this study has been widely used as inhibitor of class I and class IIa HDACs in in vivo studies (Febo et al., 2009; Rane et al., 2012). At much higher doses, *e.g.*, 1.2 g/kg, NaB may trigger a stress-like response (Gagliano et al., 2014). Moreover, in line with the previous studies (Kilgore et al., 2010; Ricobaraza et al., 2012), we did not find behavior changes after chronic treatment with NaB in control rodents. We only studied the male rats because the previous studies have shown that the male rats could be more susceptive to the developmental deficits induced by neonatal anesthesia with isoflurane, sevoflurane, or propofol (Lee et al., 2014; Rothstein et al., 2008; Tan et al., 2014; Xu et al., 2015).

Conclusion

Our results provide support for the engagement of epigenetic mechanisms, e.g., sevoflurane-initiated reduction in hippocampal histone acetylation, in mediating neonatal anesthesia with sevoflurane-induced long-term developmental neurocognitive abnormalities in rodents. These findings suggest that upregulation of epigenetic mechanisms pharmacologically using HDAC inhibitors or by enhancing environmental factors known to stimulate histone acetylation such as voluntary physical exercise (Intlekofer et al., 2013) may potentially be an effective approach to ameliorate the developmental side effects of neonatal anesthesia with sevoflurane in rodents.

Acknowledgments

This work was supported by the National Natural Science Foundation of China (grant nos. 81271216 and 81471105 to J.J.Y.) and by the National Institutes of Health (grant nos. R01GM93036 and R01NS091542 to A.E.M.).

The authors would like to thank the Animal Center of Jinling Hospital and the staffs for providing animal care during this study.

Sources of financial support: The content is solely the responsibility of the authors and does not necessarily represent the official views of the National Institutes of Health.

Abbreviations

MS	maternal separation
BDNF	brain-derived neurotrophic factor
HDAC	histone deacetylases
NaB	sodium butyrate
Sev	sevoflurane
OF	open field
MWM	Morris water maze
FC	fear conditioning
MAP2	microtubule-associated protein 2
SDS-PAGE	sodium dodecyl sulfate polyacrylamide gel electrophoresis
TBST	Tris-buffered saline and Tween 20
PBS	phosphate-buffered saline
CREB	cyclic-AMP response element binding protein
CBP	CREB binding protein

References

Alarcon JM, et al. Chromatin acetylation, memory, and LTP are impaired in CBP+/− mice: a model for the cognitive deficit in Rubinstein-Taybi syndrome and its amelioration. Neuron. 2004; 42:947–59. [PubMed: 15207239]

Baker R, et al. Altered activity in the central medial thalamus precedes changes in the neocortex during transitions into both sleep and propofol anesthesia. J Neurosci. 2014; 34:13326–35. [PubMed: 25274812]

Bannister AJ, Kouzarides T. Regulation of chromatin by histone modifications. Cell research. 2011; 21:381–95. [PubMed: 21321607]

Barichello T, et al. Sodium Butyrate Prevents Memory Impairment by Re-establishing BDNF and GDNF Expression in Experimental Pneumococcal Meningitis. Mol Neurobiol. 2015; 52:734–40. [PubMed: 25284351]

Bindu B, et al. Short-term exposure to an enriched environment enhances dendritic branching but not brain-derived neurotrophic factor expression in the hippocampus of rats with ventral subicular lesions. Neuroscience. 2007; 144:412–23. [PubMed: 17097239]

Brenes JC, et al. Differential effects of social and physical environmental enrichment on brain plasticity, cognition, and ultrasonic communication in rats. J Comp Neurol. 2015

Caccamo A, et al. CBP gene transfer increases BDNF levels and ameliorates learning and memory deficits in a mouse model of Alzheimer's disease. Proc Natl Acad Sci U S A. 2010; 107:22687–92. [PubMed: 21149712]

Chung W, et al. Sevoflurane exposure during the neonatal period induces long-term memory impairment but not autism-like behaviors. Paediatr Anaesth. 2015; 25:1033–45. [PubMed: 26095314]

Cuadrado-Tejedor M, et al. Phenylbutyrate is a multifaceted drug that exerts neuroprotective effects and reverses the Alzheimer s disease-like phenotype of a commonly used mouse model. Curr Pharm Des. 2013; 19:5076–84. [PubMed: 23448463]

Dash PK, et al. Histone deactylase inhibition combined with behavioral therapy enhances learning and memory following traumatic brain injury. Neuroscience. 2009; 163:1–8. [PubMed: 19531374]

Edwards DA, et al. Bumetanide alleviates epileptogenic and neurotoxic effects of sevoflurane in neonatal rat brain. Anesthesiology. 2010; 112:567–75. [PubMed: 20124973]

Febo M, et al. Cocaine-induced metabolic activation in cortico-limbic circuitry is increased after exposure to the histone deacetylase inhibitor, sodium butyrate. Neurosci Lett. 2009; 465:267–71. [PubMed: 19638299]

Fischer A, et al. Targeting the correct HDAC(s) to treat cognitive disorders. Trends Pharmacol Sci. 2010; 31:605–17. [PubMed: 20980063]

Fischer A, et al. Recovery of learning and memory is associated with chromatin remodelling. Nature. 2007; 447:178–82. [PubMed: 17468743]

Fontan-Lozano A, et al. Histone deacetylase inhibitors improve learning consolidation in young and in KA-induced-neurodegeneration and SAMP-8-mutant mice. Mol Cell Neurosci. 2008; 39:193–201. [PubMed: 18638560]

Franks NP, Zecharia AY. Sleep and general anesthesia. Can J Anaesth. 2011; 58:139–48. [PubMed: 21170623]

Gagliano H, et al. High doses of the histone deacetylase inhibitor sodium butyrate trigger a stress-like response. Neuropharmacology. 2014; 79:75–82. [PubMed: 24212060]

Giralt A, et al. Long-term memory deficits in Huntington's disease are associated with reduced CBP histone acetylase activity. Hum Mol Genet. 2012; 21:1203–16. [PubMed: 22116937]

Gräff J, Tsai L-H. The potential of HDAC inhibitors as cognitive enhancers. Annual review of pharmacology and toxicology. 2013; 53:311–30.

Graff J, Mansuy IM. Epigenetic codes in cognition and behaviour. Behav Brain Res. 2008; 192:70–87. [PubMed: 18353453]

Guan JS, et al. HDAC2 negatively regulates memory formation and synaptic plasticity. Nature. 2009; 459:55–60. [PubMed: 19424149]

Han XD, et al. Single sevoflurane exposure increases methyl-CpG island binding protein 2 phosphorylation in the hippocampus of developing mice. Mol Med Rep. 2015; 11:226–30. [PubMed: 25338822]

Head BP, et al. Inhibition of p75 neurotrophin receptor attenuates isoflurane-mediated neuronal apoptosis in the neonatal central nervous system. Anesthesiology. 2009; 110:813–25. [PubMed: 19293698]

Intlekofer KA, et al. Exercise and sodium butyrate transform a subthreshold learning event into long-term memory via a brain-derived neurotrophic factor-dependent mechanism. Neuropsychopharmacology. 2013; 38:2027–34. [PubMed: 23615664]

Jarome TJ, Lubin FD. Epigenetic mechanisms of memory formation and reconsolidation. Neurobiol Learn Mem. 2014; 115:116–27. [PubMed: 25130533]

Jia M, et al. Suberoylanilide hydroxamic acid, a histone deacetylase inhibitor, attenuates postoperative cognitive dysfunction in aging mice. Front Mol Neurosci. 2015; 8:52. [PubMed: 26441515]

Jiang H, et al. Depletion of CBP is directly linked with cellular toxicity caused by mutant huntingtin. Neurobiol Dis. 2006; 23:543–51. [PubMed: 16766198]

Johnson MB, et al. Functional and evolutionary insights into human brain development through global transcriptome analysis. Neuron. 2009; 62:494–509. [PubMed: 19477152]

Kellner Y, et al. The BDNF effects on dendritic spines of mature hippocampal neurons depend on neuronal activity. Front Synaptic Neurosci. 2014; 6:5. [PubMed: 24688467]

Khan S, Jena GB. Protective role of sodium butyrate, a HDAC inhibitor on beta-cell proliferation, function and glucose homeostasis through modulation of p38/ERK MAPK and apoptotic

pathways: study in juvenile diabetic rat. Chem Biol Interact. 2014; 213:1–12. [PubMed: 24530320]

Kilgore M, et al. Inhibitors of class 1 histone deacetylases reverse contextual memory deficits in a mouse model of Alzheimer's disease. Neuropsychopharmacology. 2010; 35:870–80. [PubMed: 20010553]

Lee BH, et al. Isoflurane exposure in newborn rats induces long-term cognitive dysfunction in males but not females. Neuropharmacology. 2014; 83:9–17. [PubMed: 24704083]

Lu Y, et al. Anesthetic sevoflurane causes neurotoxicity differently in neonatal naïve and Alzheimer disease transgenic mice. Anesthesiology. 2010; 112:1404–16. [PubMed: 20460993]

McClelland S, et al. Emerging roles of epigenetic mechanisms in the enduring effects of early-life stress and experience on learning and memory. Neurobiol Learn Mem. 2011; 96:79–88. [PubMed: 21338703]

McQuown SC, et al. HDAC3 is a critical negative regulator of long-term memory formation. J Neurosci. 2011; 31:764–74. [PubMed: 21228185]

Pirooznia SK, Elefant F. Targeting specific HATs for neurodegenerative disease treatment: translating basic biology to therapeutic possibilities. Front cell neurosci. 2013; 7:30. [PubMed: 23543406]

Powell WT, LaSalle JM. Epigenetic mechanisms in diurnal cycles of metabolism and neurodevelopment. Hum Mol Genet. 2015; 24:R1–9. [PubMed: 26105183]

Rane P, et al. The histone deacetylase inhibitor, sodium butyrate, alleviates cognitive deficits in pre-motor stage PD. Neuropharmacology. 2012; 62:2409–12. [PubMed: 22353286]

Rappaport BA, et al. Anesthetic neurotoxicity-clinical implications of animal models. N Engl J Med. 2015; 372:796–7. [PubMed: 25714157]

Ricobaraza A, et al. Phenylbutyrate rescues dendritic spine loss associated with memory deficits in a mouse model of Alzheimer disease. Hippocampus. 2012; 22:1040–50. [PubMed: 21069780]

Roth TL, Sweatt JD. Annual Research Review: Epigenetic mechanisms and environmental shaping of the brain during sensitive periods of development. J Child Psychol Psychiatry. 2011; 52:398–408. [PubMed: 20626526]

Rothstein S, et al. Response to neonatal anesthesia: effect of sex on anatomical and behavioral outcome. Neuroscience. 2008; 152:959–69. [PubMed: 18329814]

Sakata K, et al. Role of activity-dependent BDNF expression in hippocampal-prefrontal cortical regulation of behavioral perseverance. Proc Natl Acad Sci U S A. 2013; 110:15103–8. [PubMed: 23980178]

Servick K. Biomedical Research. Researchers struggle to gauge risks of childhood anesthesia. Science. 2014; 346:1161–2. [PubMed: 25477435]

Seubert CN, et al. Developmental effects of neonatal isoflurane and sevoflurane exposure in rats. Anesthesiology. 2013; 119:358–64. [PubMed: 23619170]

Sharma SK. Protein acetylation in synaptic plasticity and memory. Neurosci Biobehav Rev. 2010; 34:1234–40. [PubMed: 20219532]

Shen X, et al. Selective anesthesia-induced neuroinflammation in developing mouse brain and cognitive impairment. Anesthesiology. 2013; 118:502–15. [PubMed: 23314110]

Shih J, et al. Delayed environmental enrichment reverses sevoflurane-induced memory impairment in rats. Anesthesiology. 2012; 116:586–602. [PubMed: 22354242]

Singh MD, et al. Drosophila Myc, a novel modifier suppresses the poly(Q) toxicity by modulating the level of CREB binding protein and histone acetylation. Neurobiol Dis. 2014; 63:48–61. [PubMed: 24291519]

Sun L. Early childhood general anaesthesia exposure and neurocognitive development. British journal of anaesthesia. 2010; 105(Suppl 1):i61–8. [PubMed: 21148656]

Tan S, et al. Endocrine and neurobehavioral abnormalities induced by propofol administered to neonatal rats. Anesthesiology. 2014; 121:1010–7. [PubMed: 24992523]

Vorhees CV, Williams MT. Morris water maze: procedures for assessing spatial and related forms of learning and memory. Nat Protoc. 2006; 1:848–58. [PubMed: 17406317]

Wang G, et al. Scriptaid, a novel histone deacetylase inhibitor, protects against traumatic brain injury via modulation of PTEN and AKT pathway : scriptaid protects against TBI via AKT. Neurotherapeutics. 2013a; 10:124–42. [PubMed: 23132328]

Wang SQ, et al. Neonatal sevoflurane anesthesia induces long-term memory impairment and decreases hippocampal PSD-95 expression without neuronal loss. Eur Rev Med Pharmacol Sci. 2013b; 17:941–50. [PubMed: 23640442]

Wilder RT, et al. Early exposure to anesthesia and learning disabilities in a population-based birth cohort. Anesthesiology. 2009; 110:796–804. [PubMed: 19293700]

Xu C, et al. Anesthesia with sevoflurane in neonatal rats: Developmental neuroendocrine abnormalities and alleviating effects of the corticosteroid and Cl(-) importer antagonists. Psychoneuroendocrinology. 2015; 60:173–81. [PubMed: 26150359]

Zhang MQ, et al. Neurobehavioural abnormalities induced by repeated exposure of neonatal rats to sevoflurane can be aggravated by social isolation and enrichment deprivation initiated after exposure to the anaesthetic. Br J Anaesth. 2015; 115:752–60. [PubMed: 26475803]

Highlights

- Early life exposure to sevoflurane anesthesia deteriorates neurocognitive development.
- Neonatal sevoflurane anesthesia down-regulates hippocampal histone acetylation.
- Down-regulation of histone acetylation results in impairments of hippocampal synaptic plasticity.
- Sodium butyrate, an HDAC inhibitor, may represent a promising path to safer neonatal anesthesia with sevoflurane in rodents.

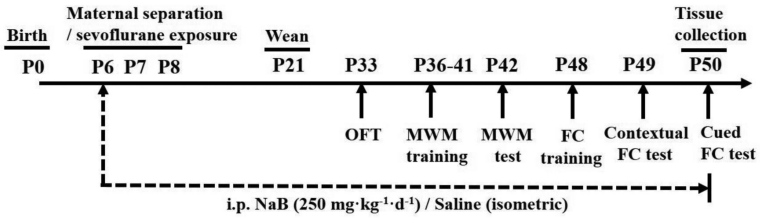

Fig. 1.
Illustration of the experimental protocol. See text for details.

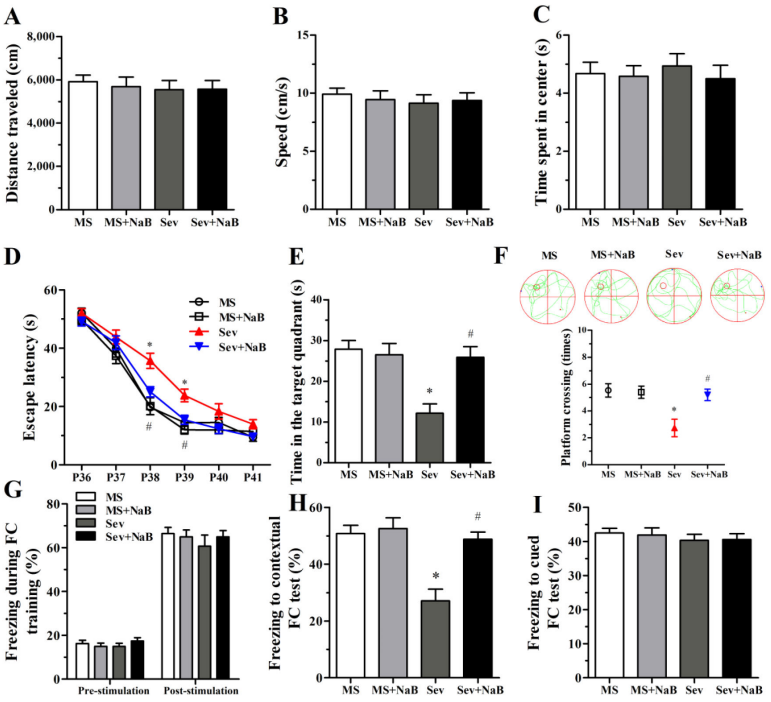

Fig. 2.

Effects of neonatal exposure to sevoflurane on behavior of rats in the open field (OF), Morris water maze (MWM), and fear conditioning (FC) tests. (A-C) Histograms showing distance traveled, speed, and time spent in center during the OF test. (D) Plots showing escape latency during the MWM training. (*$P < 0.001$ vs. the MS group; #$P = 0.007$ vs. the Sev group; P39: *$P < 0.001$ vs. the MS group; #$P = 0.018$ vs. the Sev group). (E) Histogram showing time spent in the target quadrant during the MWM test (*$P < 0.001$ vs. the MS group; #$P = 0.001$ vs. the Sev group). (F) Swimming tracks and plots showing rats crossing the escape platform during the MWM test (*$P = 0.002$ vs. the MS group; #$P = 0.007$ vs. the Sev group). (G) Histograms showing the percent of freezing during the FC training session. (H) Histograms showing the percent of freezing during the contextual FC test (*$P < 0.001$ vs. the MS group; #$P < 0.001$ vs. the Sev group). (I) Histograms showing the percent of freezing during the cued FC test. n = 15 per treatment group. MS: maternal separation; Sev: sevoflurane.

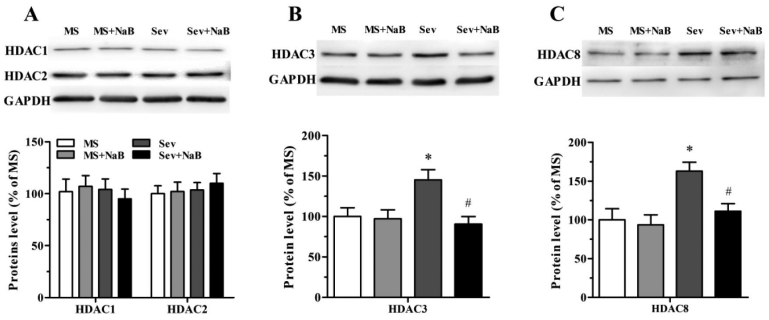

Fig. 3.

Effects of neonatal exposure to sevoflurane and sodium butyrate (NaB) treatment on expression of hippocampal class I histone deacetylases (HDACs). (A, top) Representative Western blot images of HDAC1, HDAC2, and GADPH blots in the hippocampal tissue of rats from four treatment groups. (A, bottom) Histograms showing results of the densitometric analysis of HDAC1 and HDAC2 blots in the hippocampal tissue from four treatment groups. Densities of HDAC1 and HDAC2 blots in the MS groups were taken as 100%. (B) The Western blot data for HDAC3 in the hippocampal tissue from four treatment groups presented as in (A). $^{*}P = 0.044$ vs. the MS group; $^{\#}P = 0.013$ vs. the Sev group. (C) The Western blot data for HDAC8 in the hippocampal tissue from four treatment groups presented as in (A). $^{*}P = 0.012$ vs. the MS group; $^{\#}P = 0.040$ vs. the Sev group. n = 5 per treatment group. MS: maternal separation; Sev: sevoflurane.

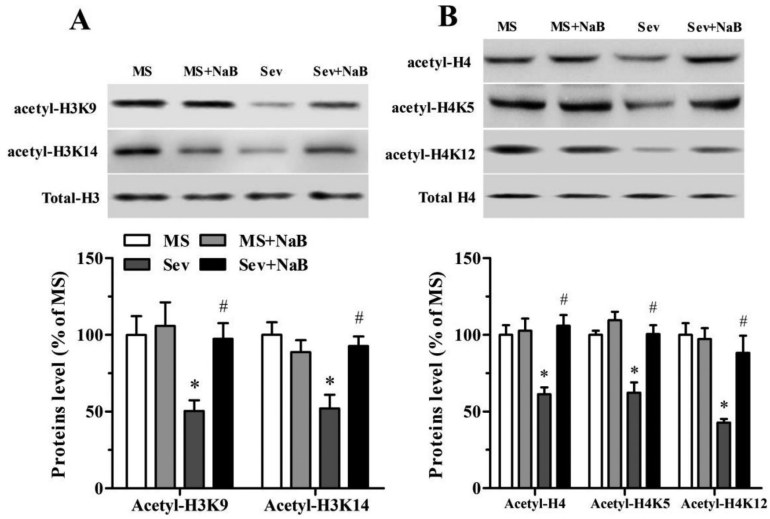

Fig. 4.

Effects of neonatal exposure to sevoflurane and sodium butyrate (NaB) treatment on expression of hippocampal acetylated histones H3 and H4. (A, top) Representative Western blot images of acetyl-H3K9, acetyl-H3K14, and total H3 blots in the hippocampal tissue of rats from four treatment groups. (A, bottom) Histograms showing results of the densitometric analysis of acetyl-H3K9 and acetyl-H3K14 blots in the hippocampal tissue from four treatment groups. Densities of acetyl-H3K9 and acetyl-H3K14 blots in the MS groups were taken as 100%. Acety-H3K9: $^{*}P = 0.036$ vs. the MS group; $^{\#}P = 0.048$ vs. the Sev group. Acetyl-H3K14: $^{*}P = 0.003$ vs. the MS group; $^{\#}P = 0.010$ vs. the Sev group. (B) The Western blot data for acetyl-H4, acetyl-H4K5, and acetyl-H4K12 in the hippocampal tissue from four treatment groups presented as in (A). Acetyl-H4: $^{*}P = 0.004$ vs. the MS group; $^{\#}P = 0.001$ vs. the Sev group. Acetyl-H4K5: $^{*}P = 0.001$ vs. the MS group; $^{\#}P = 0.001$ vs. the Sev group. Acetyl-H4K12: $^{*}P < 0.001$ vs. the MS group; $^{\#}P = 0.004$ vs. the Sev group. n = 5 per treatment group. MS: maternal separation; Sev: sevoflurane.

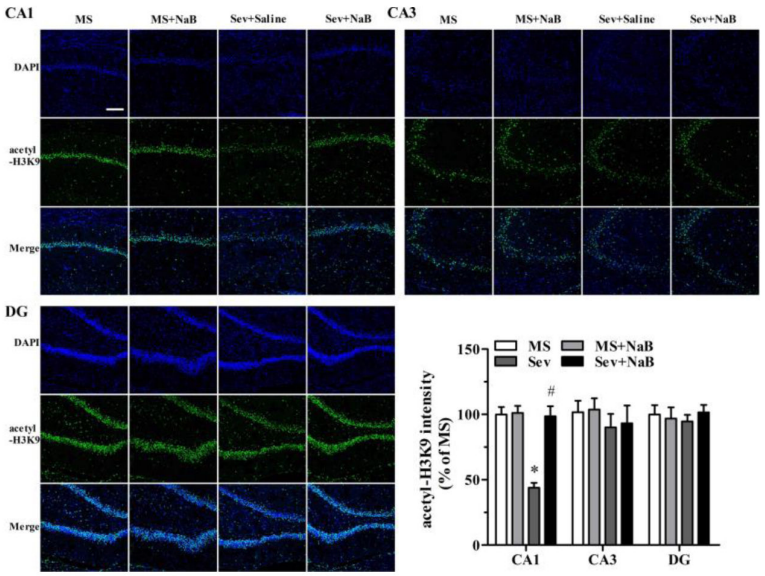

Fig. 5.

Effects of neonatal exposure to sevoflurane and sodium butyrate (NaB) treatment on the intensity of acetyl-H3K9 in hippocampal subfields. Representative images of the hippocampal CA1, CA3, and dentate gyrus (DG) areas of the rats from four groups: 4',6-diamidino-2-phenylindole (DAPI), acetyl-H3K9, and an overlay of DAPI and acetyl-H3K9 images. The intensity of acetyl-H3K9 in hippocampal CA1 (*$P < 0.001$ vs. the MS group; $^{\#}P < 0.001$ vs. the Sev group), CA3, and DG areas. The intensity of acetyl-H3K9 in the group was taken as 100%. n = 6 per treatment group. Scale bar = 50 μm. MS: maternal separation; Sev: sevoflurane.

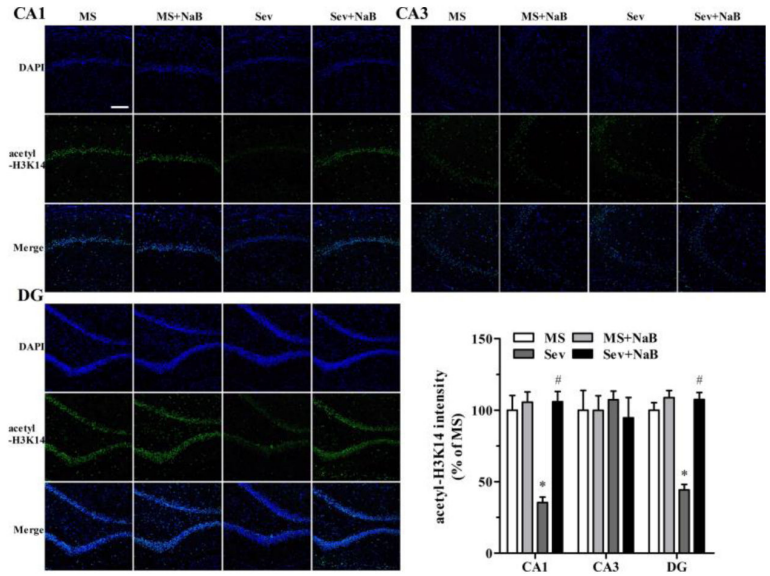

Fig 6.

Effects of neonatal exposure to sevoflurane and sodium butyrate (NaB) treatment on the intensity of acetyl-H3K14 in hippocampal subfields. Representative images of the hippocampal CA1, CA3, and dentate gyrus (DG) areas of the rats from four treatment groups: 4',6-diamidino-2-phenylindole (DAPI), acetyl-H3K14, and an overlay of DAPI and acetyl-H3K14 images. The intensity of acetyl-H3K14 in hippocampal CA1: $^{*}P < 0.001$ vs. the MS group; $^{\#}P < 0.001$ vs. the Sev group. DG: $^{*}P < 0.001$ vs. the MS group; $^{\#}P < 0.001$ vs. the Sev group. The intensity of acetyl-H3K14 in the MS group was taken as 100%. n = 6 per treatment group. Scale bar = 50 μm. MS: maternal separation; Sev: sevoflurane.

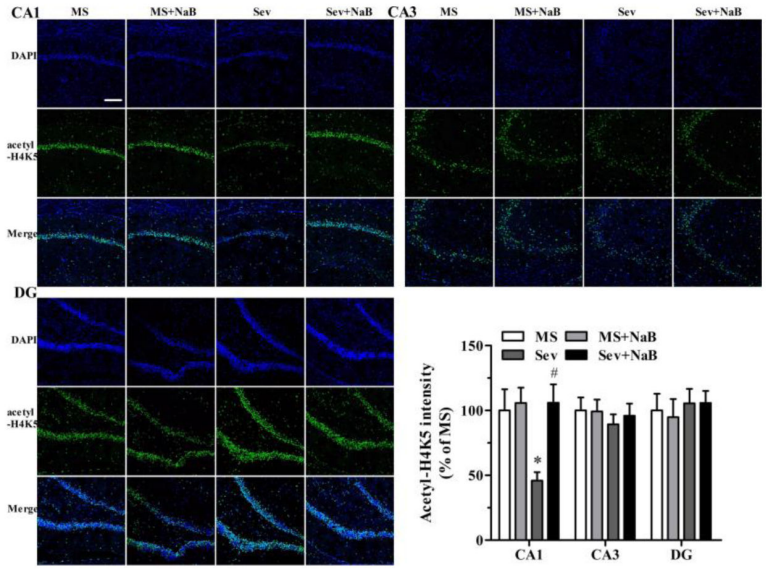

Fig. 7.

Effects of neonatal exposure to sevoflurane and sodium butyrate (NaB) treatment on intensity of acetyl-H4K5 in different hippocampal subfields. Representative images of the hippocampal CA1, CA3, and dentate gyrus (DG) areas of the rats from four treatment groups: 4',6-diamidino-2-phenylindole (DAPI), acetyl-H4K5 and an overlay of DAPI and acetyl-H4K5 images. The intensity of H4K5 acetylation in hippocampal CA1 (*P = 0.032 vs. the MS group; $^{\#}P$ = 0.016 vs. the Sev group), CA3, and DG subfields. The intensity of acetyl-H4K5 in the MS group was taken as 100%. n = 6 per treatment group. Scale bar = 50 μm. MS: maternal separation; Sev: sevoflurane.

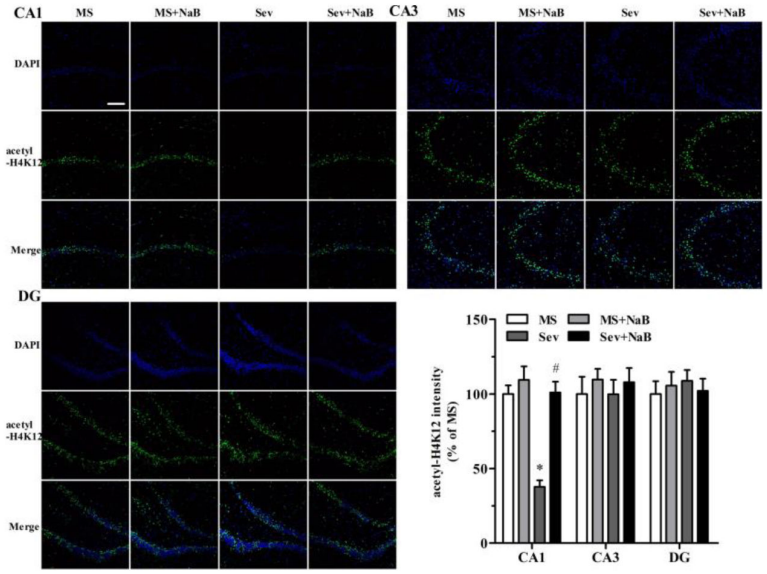

Fig 8.

Effects of neonatal exposure to sevoflurane and sodium butyrate (NaB) treatment on intensity of acetyl-H4K12 in different hippocampal subfields. Representative images of the hippocampal CA1, CA3, and dentate gyrus (DG) areas of the rats from four treatment groups: 4',6-diamidino-2-phenylindole (DAPI), acetyl-H4K5 and an overlay of DAPI and acetyl-H4K12 images. The intensity of acetyl-H4K12 in hippocampal CA1: $^{*}P < 0.001$ vs. the MS group; $^{\#}P < 0.001$ vs. the Sev group). The intensity of acetyl-H4K12 in the MS group was taken as 100%. n = 6 per treatment group. Scale bar = 50 μm. MS: maternal separation; Sev: sevoflurane.

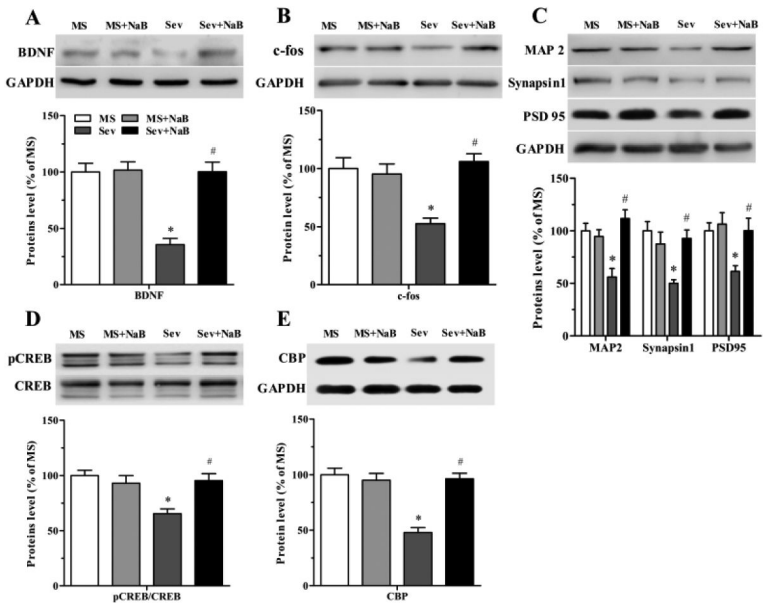

Fig. 9.

Effects of neonatal exposure to sevoflurane and sodium butyrate (NaB) treatment on expression of hippocampal proteins. (A) (A, top) Representative Western blot images of brain-derived neurotrophic factor (BDNF) and GADPH blots in the hippocampal tissue of rats from four treatment groups. (A, bottom) Histograms showing results of the densitometric analysis of BDNF in the hippocampal tissue from four treatment groups. Densities of BDNF blots in the MS group were taken as 100%. $^{*}P < 0.001$ vs. the MS group; $^{\#}P < 0.001$ vs. the Sev group. (B) Western blot data for c-fos in the hippocampal tissue from four treatment groups presented as in (A). $^{*}P = 0.012$ vs. the MS group; $^{\#}P = 0.001$ vs. the Sev group. (C) Western blot data for microtubule-associated protein 2 (MAP2), synapsin 1, and PSD 95 in the hippocampal tissue from four treatment groups presented as in (A). MAP2: $^{*}P = 0.004$ vs. the MS group; $^{\#}P < 0.001$ vs. the Sev group. Synapsin 1: $^{*}P = 0.004$ vs. the MS group; $^{\#}P = 0.0012$ vs. the Sev group. PSD95: $^{*}P = 0.043$ vs. the MS group; $^{\#}P = 0.042$ vs. the Sev group. (D) Western blot data for pCREB/CREB in the hippocampal tissue from four treatment groups presented as in (A). $^{*}P = 0.002$ vs. the MS group; $^{\#}P = 0.008$ vs. the Sev group (E) Western blot data for CBP in the hippocampal tissue from four treatment groups presented as in (A). $^{*}P < 0.001$ vs. the MS group; $^{\#}P < 0.001$ vs. the Sev group. n = 5 per treatment group. MS: maternal separation; Sev: sevoflurane.

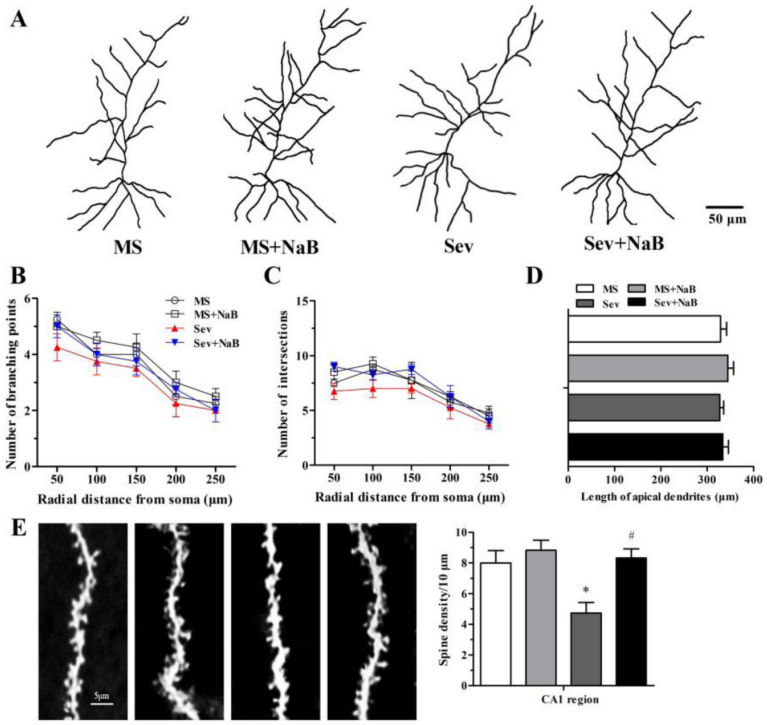

Fig. 10.

Effects of neonatal exposure to sevoflurane and sodium butyrate (NaB) treatment on synaptic branching and dendritic spine in the hippocampal CA1 subfield. (A) Representative camera tracings of hippocampal CA1 pyramidal neurons from the four groups. (B and C) Histograms showing the dendritic branching points, intersections, and the length of apical branching in hippocampal CA1 pyramidal neurons. (D) Histograms showing the number of dendritic spines in hippocampal CA1 subfield (*P = 0.027 vs. the MS group; $^{\#}P$ = 0.015 vs. the Sev group). n = 4 per treatment group. Scale bar = 5 μm. MS: maternal separation; Sev: sevoflurane.